This is an open access article published under a Creative Commons Attribution (CC-BY) License, which permits unrestricted use, distribution and reproduction in any medium, provided the author and source are cited.

ACS AUTHORCHOICE

Biomacromolecules

pubs.acs.org/Biomac

Article

Fabrication of Biohybrid Cellulose Acetate-Collagen Bilayer Matrices as Nanofibrous Spongy Dressing Material for Wound-Healing Application

Giriprasath Ramanathan, Liji Sobhana Seleenmary Sobhanadhas, Grace Felciya Sekar Jeyakumar, Vimala Devi, Uma Tiruchirapalli Sivagnanam,* and Pedro Fardim*

Cite This: *Biomacromolecules* 2020, 21, 2512−2524

Read Online

ACCESS | Metrics & More | Article Recommendations | Supporting Information

ABSTRACT: Tissue engineering is currently one the fastest growing engineering fields, requiring fabrication of advanced and multifunctional materials to be used as scaffolds or dressing for tissue regeneration. In this work, a bilayer matrix was fabricated by electrospinning of a hybrid cellulose acetate nanofibers (CA) containing bioactive latex or Ciprofloxacin over highly interconnected collagen (CSPG) 3D matrix previously obtained by a freeze-drying process. The bilayer matrix was fabricated with a nanofibrous part as the primary (top) layer and a spongy porous part as the secondary (bottom) layer by combining electrospinning and freeze-drying techniques to enhance the synergistic effect of both materials corresponding to physical and biological properties. The final material was physicochemically characterized using Fourier transform infrared spectroscopy (FTIR), and scanning electron microscopy (SEM). The bilayer matrix exhibited nanofibrous and 3D porous structure with properties such as high porosity, swelling, and stability required for soft-tissue-engineering applications. Furthermore, the *in vitro* biological and fluorescence properties of the matrix were tested against NIH 3T3 fibroblast and human keratinocyte (HaCaT) cell lines and showed good cell adhesion and proliferation over the bilayer matrix. Thus, the synergistic combination of nanofibrous material deposition onto to the collagenous porous material has proved efficient in the fabrication of a bilayer matrix for skin-tissue-engineering applications.

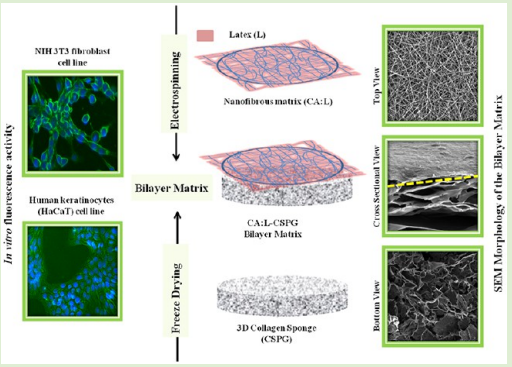

1. INTRODUCTION

Wound healing is a physiological process of repair, restoration, and regeneration of the damaged skin tissues or cells due to external injury or accidents. The increasing occurrence of nonhealing wounds have aided the development of new wound-dressing materials for tissue-engineering applications.[1] The need for a therapeutic product with multifunctional properties for tissue engineering has been reported widely in the development of biomaterials. The dressing material mimics the structural function of an extracellular matrix (ECM) providing a substrate with the ability for migration and proliferation of cells during wound healing. Different fabrication techniques can be used for producing dressing materials including casting, electrospinning, and sponge preparation via freeze-drying. Electrospinning is a versatile process for the fabrication of nanofibrous scaffolds for tissue engineering,[2] while freeze-drying is an attractive approach for the development of a unique material with 3D architecture and porous matrix for wound healing.[3] This 3D porous nanofibrous scaffold has flexibility, high surface-to-volume ratio, excellent biocompatibility, and porous morphology for oxygen permeability to serve as a prominent biomaterial for wound healing.[4] The design of an excellent biomaterial involves not only the selection of a suitable polymer but also the choice of the fabrication techniques to produce a 3D material with synergistic effects of bioactivity combined with micro and nanohierarchical architectures that enhance the cell−material interactions.[5,6] In recent years, research focuses on understanding the functions and fabrication of ECM-mimicking sustainable biomaterials with well-constructed and guided structures and well-defined material properties, stability, and biological properties for tissue regeneration.[7] Tochobanian et al. examined several papers published in the last two decades with the application of polysaccharides in the field of tissue engineering and identified a growing interest in polysaccharides like chitosan, alginate, hyaluronan, and cellulose as an implant or biomaterial in tissue-engineering applications.[8]

The conceptualization of design of the bilayer matrix with electrospinning and freeze-drying approach was configured to develop a nanofibrous spongy morphology as a hybrid wound-dressing

Received: April 7, 2020
Revised: April 27, 2020
Published: April 28, 2020

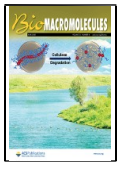

ACS Publications

© 2020 American Chemical Society

https://dx.doi.org/10.1021/acs.biomac.0c00516
Biomacromolecules 2020, 21, 2512−2524

material. The top layer of the bilayer construct provides the native architecture with a high surface-to-volume ratio to enhance the cell attachment, and proliferation.[9] Additionally, the bottom layer of the bilayer construct supports the migration of fibroblasts and absorption of exudates, and it provides a moist environment with good gaseous exchange for effective healing of wounds.[10] The assessment of the bilayer matrix with above-mentioned properties can be obtained only with selection hybrid material combination and fabrication process. The combination of the polysaccharide and the proteinaceous material as a nanofibrous spongy bilayer matrix will develop an ideal wound-dressing material with desired physical and biological properties to mimic the function of the extracellular matrix and its architecture.[11]

The functionalization of the phospholipid bilayer with the decellularized extracellular matrix as a hybrid biomimetic interface supports the proliferation and attachment of cells.[12] However, the decellularized or the acellular matrix resembles the three-dimensional structure of the spongy material fabricated with freeze-drying technique.[12,13] In our previous study on the evaluation of the nanofibrous matrix over the film[14] and 3D sponge[11] as a durable bilayer matrix exhibited with better integrity of the material for the effective healing of wounds.

Cellulose acetate (CA) is a polysaccharide derivative which has been used for the development of biomaterial for various biomedical and tissue-engineering applications.[15] This biopolymer provides excellent biocompatibility, biodegradability and has the potential to enhance the cellular interaction between the scaffold and the fibroblast cells.[16,17] Collagen attracts attention because of its good permeability, biocompatibility, biodegradability, low immunogenicity, and creation of good interactions between the cells due to stimulation of specific cell-morphology phenotypes.[18−20] However, many researchers prefer marine collagen as the alternative to mammalian collagen due to the low risk of transmission of infection to humans and also far less associated with religious belief on human usage of marine-derived health care products.[21,22] The prior mentioned polysaccharide and proteinaceous material have desirable traits exclusive of each other and none of the scaffolds alone cannot attain the whole desired physical and biological property when its used as separate layer.

Calotropis procera (Asclepiadaceae), commonly known as milkweed is a traditionally significant medicinal plant widely used as folk medicine in India for dermal disorders, antimicrobial actions, and pain relief or anti-inflammatory agents.[23] The latex from *C. procera* is a natural plant polymer secreted by the ducts of the lacticiferous tissue.[24] The latex from *C. procera* is mainly a complex mixture of secondary metabolites,[25] phytochemicals,[26] and antioxidants.[27] Moreover, the bioactive latex from the aerial parts of *C. procera* plant has been used as traditional medicine in the past for wound healing.[28] In this work, the bioactive latex (L) from *C. procera* was incorporated via electrospinning into CA nanofiber to produce a biohybrid nanomaterial (CA:L) that was deposited onto a bilayer 3D collageneous porous sponge (CSPG) to be used as a bilayer wound-dressing material (CA:L-CSPG). The resulting bioactive nanofibrous and spongy matrix is expected to improve the absorption of wound exudates, cell adhesion, and cell proliferation, while the biohybrid CA:L acts as antimicrobial agent. On the basis of these goals, we hypothesized that a synergistic effect of bioactivity and fibrillar and porous bioshapes could be used as suitable material for cell adhesion and proliferation and lead to a potential application in regenerative dressing material for wound care management.

2. MATERIALS AND METHODS

Arothron stellatus fish were collected from the deep sea in the Bay of Bengal region near coastal side of Nagapattinam, Tamilnadu, India. Fresh latex of *C. procera* was collected from Chennai, Tamilnadu, India. Cellulose acetate (average molecular weight ∼30 000 by GPC), Tris-HCl, Tris buffer, Glycine, Dulbecco's modified Eagle's medium (DMEM), fetal bovine serum (FBS), and supplementary antibiotics for tissue culture were purchased from Sigma-Aldrich, India. The mouse NIH 3T3 fibroblast and human keratinocytes cell lines (HaCaT) were obtained from the National Centre for Cell Science (NCCS), Pune, India. All the other chemicals and culture wares were purchased from Sigma-Aldrich unless specified otherwise.

2.1. Extraction of Latex (L) from *Calotropis procera*. Fresh latex (L) of *C. procera* was collected from the aerial parts of the healthy plants in a glass container containing distilled water 1:1 v/v. The mixture was gently transported to the laboratory without disturbing the homogeneity and was stored at 4 °C. Further, the supernatant was decanted and centrifuged at 14 000 rpm/30 min/25 °C. The clear supernatant was decanted and dialyzed extensively against deionized water using a dialysis bag (12000 Da) for 24 h at 25 °C.[28] Finally, the dialysate was freeze-dried and stored at room temperature.

2.1.1. In Vitro Antioxidant Assay, Hemocompatibility Assay, and Antimicrobial Activity of Latex (L) from Calotropis procera. The *in vitro* antioxidant studies (DPPH radical-scavenging activity,[29] reducing power assay,[30] hydrogen peroxide scavenging activity,[31] and antimicrobial activity of the *C. procera* latex extracts were studied as per the standard methods. The *C. procera* latex solution was prepared by dissolving 50 mg of freeze-dried latex in 10 mL water and stirring for 8 h to get uniform homogenized latex solution. For the evaluvation of the antioxidant and antimicrobial activity, 500 μL of the dissolved extract was used.

The hemolysis assay was carried out to determine whether the extracted latex is hemocompatible with fresh blood when used for *in vivo* application. Whole blood was collected, heparinized, and diluted using PBS. Various concentration of latex was added and incubated at 37 °C in an incubator shaker for 2 h. The volume was made up to 1 mL using PBS. Blood treated with 500 μL of Triton X-100 and PBS was used as positive and negative control, respectively. After incubation, the samples were centrifuged at 5000 rpm for 10 min and the absorbance of the supernatants was read at 540 nm. Hemolytic percentage is calculated using the following formula

$$\%\text{hemolysis} = \frac{A_S - A_{NC}}{A_{PC} - A_{NC}} \times 100 \quad (1)$$

where A_S is the absorbance of test sample and A_{PC} and A_{NC} are the absorbance values of positive and negative controls, respectively.[32]

The antimicrobial activity of the Latex (L) was evaluated against *Staphylococcus aureus* (ATCC 11632, Gram-positive) and *Pseudomonas aeruginosa* (ATCC 10145, Gram-negative) using modified well diffusion method. About 100 μL [10^5 CFU (colony forming units)]) of each microbial suspension was distributed over the surface of Muller−Hinton agars using a sterile glass spreader. Further, the well was created, and 500 μL of the dissolved extract was transferred inside the well and the plates were incubated at 37 °C for 24 h. The antibacterial activity was indicated with the presence of inhibition zone around against the test organism.[33,10]

2.2. Fabrication of Collagen Sponge 3D Architectures (CSPG). The collagen from the fish of marine origin was extracted following our previous study.[34] The highly interconnected spongy 3D matrix that was fabricated with help of step by step freeze-drying method showed better swelling index and porosity. Moreover, the advantage of the 3D matrix with nanofibrous matrix supports the fabrication of unique bilayer matrix for tissue-engineering application. Briefly, 30 mL of 2% w/v collagen solution in 0.1 M acetic acid was mixed uniformly at 24 000 rpm/10 min/4 °C. Then, well homogenized collagen solution was transferred to a Teflon template and was kept in a freezer for step by step freezing process from −4, −20, −40, and −80 °C, respectively, at constant time intervals for 24 h. Further, the frozen samples were kept at freeze-dryer with −80 °C under a vacuum

https://dx.doi.org/10.1021/acs.biomac.0c00516
Biomacromolecules 2020, 21, 2512−2524

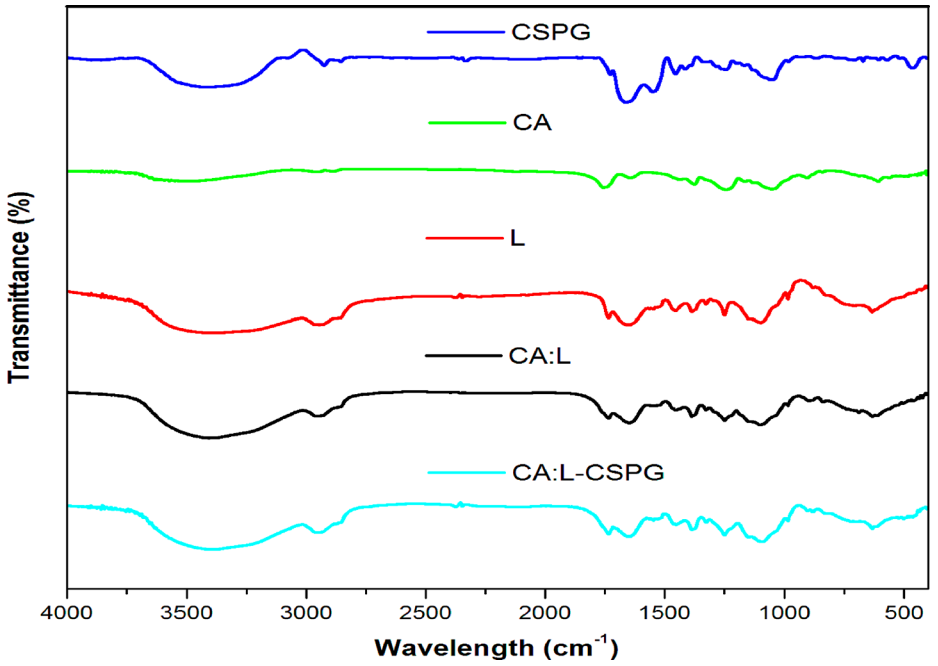

Figure 1. (a) Fourier Transform Infrared spectra (FTIR) of the matrix.

of 0.1 mbar for 72 h in the freeze-dried to get CSPG spongy matrix. All the preparative procedure was performed in a cold room maintained at 4 °C. Moreover, the step-by-step freezing initiate will enhance the formation of new ice crystals in the surrounding aqueous solution and thereby increasing the interconnectivity of the collagen scaffolds with pore size and porosity to get the 3D dimensional structure of the spongy collagen.[3]

2.3. Electrospinning of Bilayer Nanofibrous 3D Spongy Matrix. Different concentrations of CA polymer solutions were prepared by dissolving 0.4, 0.5, and 0.6 g of CA in 10 mL of acetone at constant stirring for 12 h until the mixture was clear and viscous. These uniform solutions of CA (4, 5, and 6% (w/v)) were electrospun over grounded aluminum substrate, placed at a distance of 15 cm perpendicular to 24G needle connected to the positive terminal of a high-voltage DC power supply (ESPIN-NANO electrospinning apparatus). The polymer solution was extracted with 1 mL/h using a controlled syringe pump subjected to an electric potential of 4 kV/cm. Furthermore, the latex (L) was incorporated into the CA matrix by adding 50 mg of L in 10 mL of CA solution and was stirred for 12 h to get uniform homogenized solution. The well-blended CA:L solution was electrospun over the fabricated CSPG spongy matrix placed over the grounded aluminum substrate and electrospun with above parameters to obtain bilayer nanofibrous 3D spongy matrix (CA:L-CSPG). Similarly, Ciprofloxacin (D) incorporated CA:D-CSPG bilayer matrix was fabricated in the same way. The fabricated bilayer matrix was sterilized using ethylene oxide and stored at room temperature until further use.[11]

2.4. FTIR, SEM, AFM, and Contact-Angle Analyses. The bilayer matrix was characterized using FTIR to identify any formation or changes in the functional groups. The spectral measurements were measured at a resolution of 4 cm^{-1} in the frequency range of 4000−500 cm^{-1} using ABB 3000 FTIR spectrometer. The top, bottom, and cross-sectional morphology of fabricated bilayer matrices (CA-CSPG and CA:L-CSPG) were analyzed by SEM (JEOL JSM-6460 LV and F E I Quanta FEG 200 - HRSEM). The samples were coated with gold to enhance the surface conductivity before scanning.[10,35] Static water-contact-angle measurements were performed to investigate the hydrophilicity of the electrospun nanofibrous matrices. Ultrapure deionized water (10 μL) was dropped using a microsyringe on the surface of the dried matrices, and the contact angle was measured by sessile drop method at room temperature using Holmarc Opto-Mechatronics Contact angle meter, India (Version 8.0). The process was repeated at three points per sample and the images taken were analyzed using computer-interfaced software.[15]

2.5. Swelling Study. The swelling ability of the CA-CSPG and CA:L-CSPG bilayered matrix (1 × 1 cm) was studied by swelling of the matrix in a phosphate buffer solution (PBS, pH 7.4) at 37 °C. The swollen matrix was collected at different time intervals, superficially dried with filter paper, and weighed on an analytical microbalance. The percentage of swelling Sw(%) of the bilayered matrix was calculated according to the following equation.

$$\mathrm{Sw}(\%) = \frac{W_s - W_o}{W_o} \times 100 \tag{2}$$

where W_s is the weight of the matrix at the equilibrium of swelling at each time evaluated, and W_o denotes the initial weight of the matrix.[21]

2.6. Porosity. The porosity of the fabricated bilayer scaffold was determined via the liquid displacement method using ethanol as the displacement liquid due to its easy penetration through the pores of the scaffolds, which will not induce shrinking or swelling as a nonsolvent of the polymers.[36] A known weight (W) of the sample was immersed in a graduated cylinder containing a known volume (V_1) of ethanol. The samples were kept in ethanol for 5 min, and then a series of brief evacuation−repressurization cycles were conducted to force the ethanol into the pores of the scaffold. The process was repeated until the air bubbles stopped. The total volume of the ethanol and the ethanol-impregnated scaffolds was then recorded as V_2. The difference in the volume was calculated by (V_2−V_1). The scaffolds impregnated with ethanol were removed from the cylinder, and the residual ethanol volume was recorded as V_3. The porosity of the scaffolds was obtained using the following equation[37]

$$\text{porosity} = \frac{V_1 - V_S}{V_2 - V_S} \tag{3}$$

2.7. *In Vitro* Enzymatic Degradation. *In vitro* enzymatic degradation of the bilayered matrix was determined by noting the weight change at regular time intervals, upon incubation with collagenase from *Clostridium histolyticum*. Briefly, a known weight of each sample (CA, CA:L, CSPG, CA-CSPG, and CA:L-CSPG matrix) were taken in triplicates and dried overnight. Then, 100 units per mL of collagenase was added to all the test samples and incubated for 24 h at 37 °C. After the completion of the incubation time, the samples were centrifuged, freeze-dried, and then weighed. The extent of

https://dx.doi.org/10.1021/acs.biomac.0c00516
Biomacromolecules 2020, 21, 2512−2524

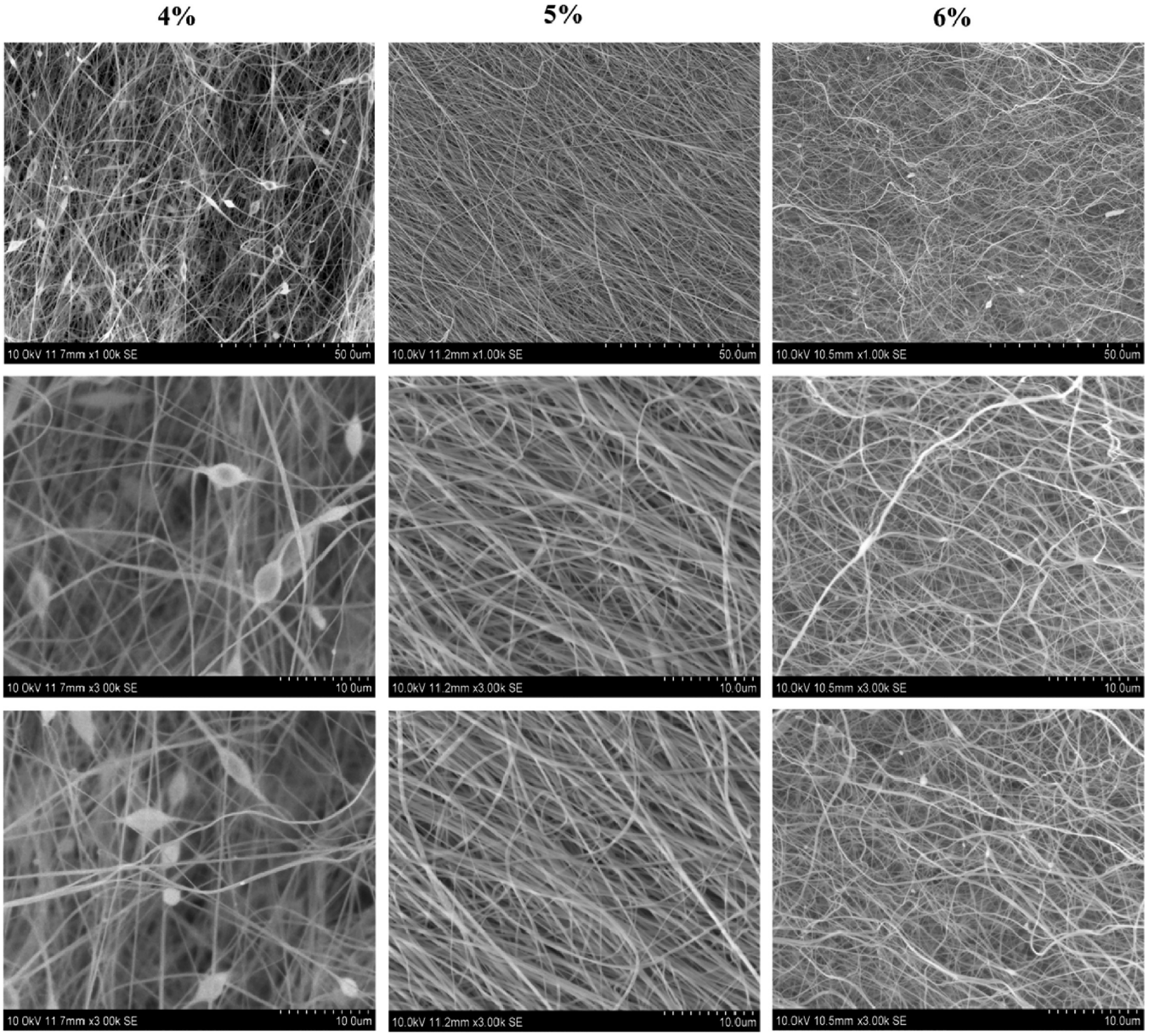

Figure 2. Scanning electron microscopy (SEM) of cellulose acetate nanofibers (4, 5, and 6 wt %).

biodegradation of the matrix was determined gravimetrically through the weight loss.[33]

2.8. *In Vitro* Drug Release Study. The *in vitro* quantification of drug release from the CA:L-CSPG and CA:D-CSPG bilayer matrix was studied using Franz-type diffusion cell apparatus. The bilayered matrix with drug was placed into the diffusion apparatus and incubated with phosphate buffer solution (PBS, pH 7.4) at 37 °C in the receiver compartment. At predetermined time intervals, 1 mL of the medium was removed from the receiver compartment and replaced with equal quantity fresh PBS solution to maintain constant volume. The L and ciprofloxacin (D) content in the matrix was determined by measuring the absorbance at 218 and 275 nm respectively (Shimadzu UV 1800Ver. 2.43).[10] The percentage of drug release from the scaffolds were determined using the following equation,

$$A = \frac{Q_p}{Q_t} \times 100 \tag{4}$$

where A is the percentage of drug release from scaffolds Q_p is the quantity of drug release and Q_t is the total quantity of L or D loaded in the bilayered matrix. The L and D release mechanism from the nanofibrous matrix was explained by examining several drug release kinetics models.

2.9. *In Vitro* Biocompatibility, Cell Adhesion, and Proliferation Studies of the Bilayer Matrix. The effect of the bilayer matrix on the proliferation of NIH 3T3 fibroblast andHaCaT cell lines was assessed using the MTT assay. In brief, the cells (5×10^4 cells mL^{-1}) were cultured along with DMEM medium and were grown over the CA-CSPG and CA:L-CSPG bilayer matrix in 24-well plates for 24, 48, and 72 h. Further, 100 μL of MTT solution (0.5 mg mL^{-1}) was added at each time point and the plate was incubated for at 37 °C for 4 h in a humidified atmosphere of 5% CO_2. The MTT solution was removed and 500 μL/well of dimethyl sulfoxide (DMSO) was added to solubilize the formazan crystals. Then, 100 μL of solution was taken and transferred to 96 well plate. The absorbance of the solution was measured at 570 nm using Universal Microplate Reader.[11] To observe the cell attachment and morphology over the bilayered matrix, the medium was removed, and the cells were fixed with 4% paraformaldehyde and washed several times with phosphate buffered saline (PBS). After being washed with PBS, the bilayer matrix with cells were dehydrated using series of graded ethanol solutions. Finally, the morphology of the cells was observed using SEM (JEOL JSM-6460 LV and F E I Quanta

https://dx.doi.org/10.1021/acs.biomac.0c00516
Biomacromolecules 2020, 21, 2512−2524

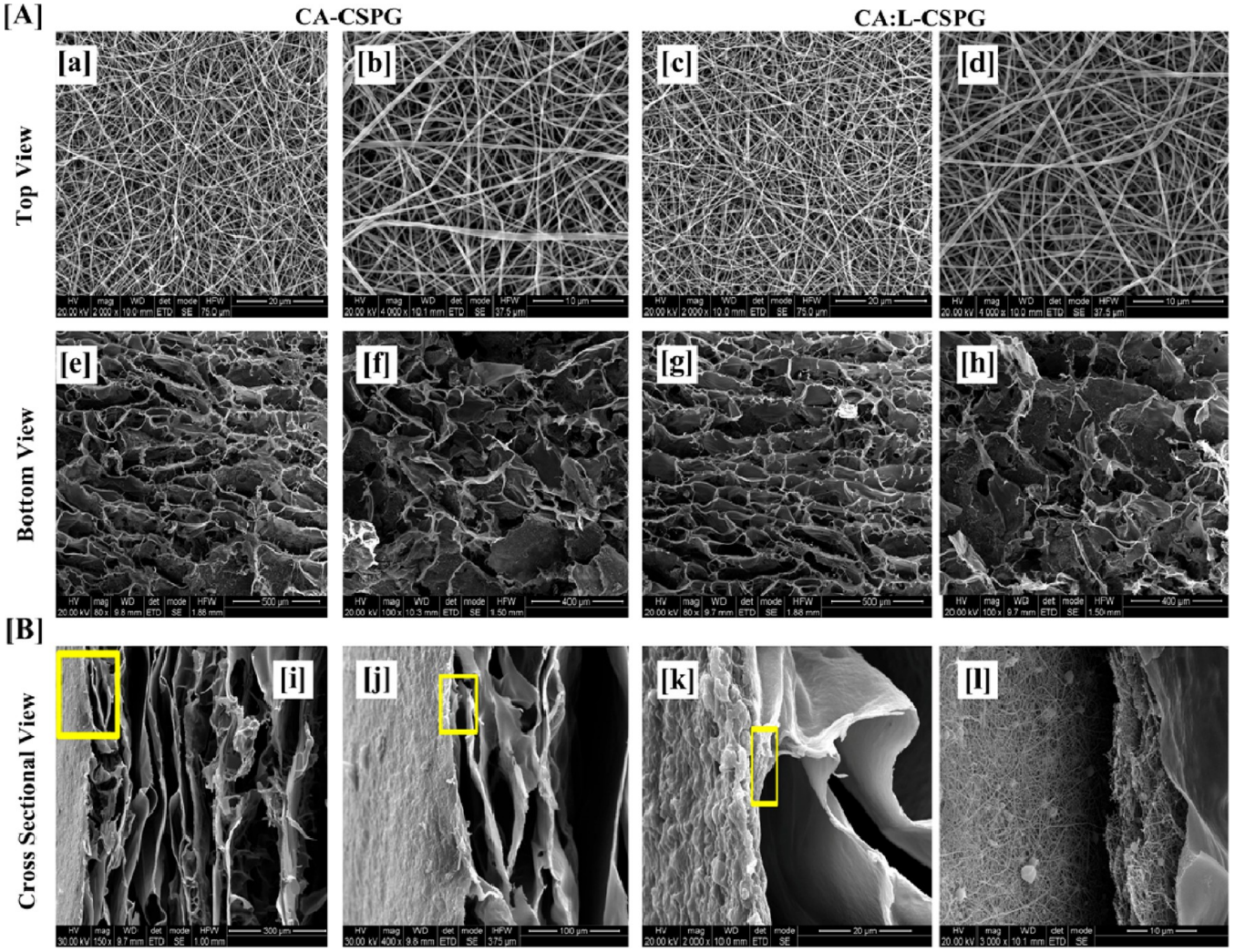

Figure 3. (A) Scanning electron microscopy (SEM) of the CA-CSPG and CA:L-CSPG bilayer matrix (a–d) top view, (e–h) bottom view of the bilayer matrix. (B) (i–l) Cross-sectional SEM micrograph of the bilayer matrix.

FEG 200 - HRSEM). *In vitro* fluorescence staining techniquee was done to visualize the attachment and proliferation of the cells over the bilayered matrix at regular time intervals (24, 48, and 72 h). The bilayered matrix was fixed with 4% paraformaldehyde and washed several times with PBS. Then the fixed cells were counterstained using DAPI (2 mg mL^{-1}) and Calcein AM (2 μM; 400 μL) and incubated (30 min, 37 °C) to visualize the cell nuclei and live cells respectively using EVOS FLoid Cell Imaging Station (EVOS FLoid Cell Imaging Station, Thermo Fisher Scientific, U.S.A.).[10]

2.10. Antimicrobial Activity. The antimicrobial activity of the CA and CA:L nanofibrous matrix (12 × 12 mm) were evaluated against *Staphylococcus aureus* (ATCC 11632, Gram-positive) and *Pseudomonas aeruginosa* (ATCC 10145, Gram-negative) using modified disc diffusion method. About 100 μL [10^5 CFU (colony forming units)]) of each microbial suspension was distributed over the surface of Muller-Hinton agars using a sterile glass spreader. Further, the respective nanofibrous matrix with and without latex (L) were place side by side and the plates were incubated at 37 °C for 24 h. The antibacterial activity was indicated with the presence of inhibition zone around against the test organism.[38,10]

2.11. Statistical Analysis. Data were expressed as the mean ± SD ($n = 3$). ANOVA (analysis of variance) and student's *t*-test were done to determine the significant differences among the groups. The observed differences were statistically significant when $p < 0.05$. All statistical analyses were performed using Graph Pad Prism software.

3. RESULTS AND DISCUSSION

3.1. FTIR Spectra. The FTIR spectra show the structural changes corresponding to the functional groups of the material in Figure 1. The spectra of the CSPG matrix show the presence of carbonyl group arising from the main structural protein collagen. The characteristic absorption peaks inferred for the triple helix structure of collagen are amide I (1600–1660 cm^{-1}), amide II (1550 cm^{-1}) and amide III (1320–1220 cm^{-1}) arising from the N–H stretching of the hydrogen bonded amide groups (Ramanathan et al., 2017).[10] The FTIR signals of the latex from the *C. procera* are observed at 1637, 1412, and 1386 cm^{-1}.[39] The CA nanofibrous matrix shows the characteristic bands such as the asymmetric C–O–C bond at 1050 cm^{-1}, C–O–C glycosidic linkage at 1159 cm^{-1} and antisymmetric bending of methyl groups in the acetate at 1374 and 1430 cm^{-1}. In addition, the stretching vibration from the C–H methylene group was observed in the range between 2800 and 3000 cm^{-1} and the wide stretching of hydroxyl groups from the polysaccharide backbone between 3050 and 3700 cm^{-1}. Moreover, CA nanofibrous matrix exhibited with no sign of residual acetone after electrospinning was evident from the Figure 1 Thus, the bilayer matrix confers all the peaks corresponding to the glyosidic linkage, symmetric C–O–C bond, the methyl

https://dx.doi.org/10.1021/acs.biomac.0c00516
Biomacromolecules 2020, 21, 2512–2524

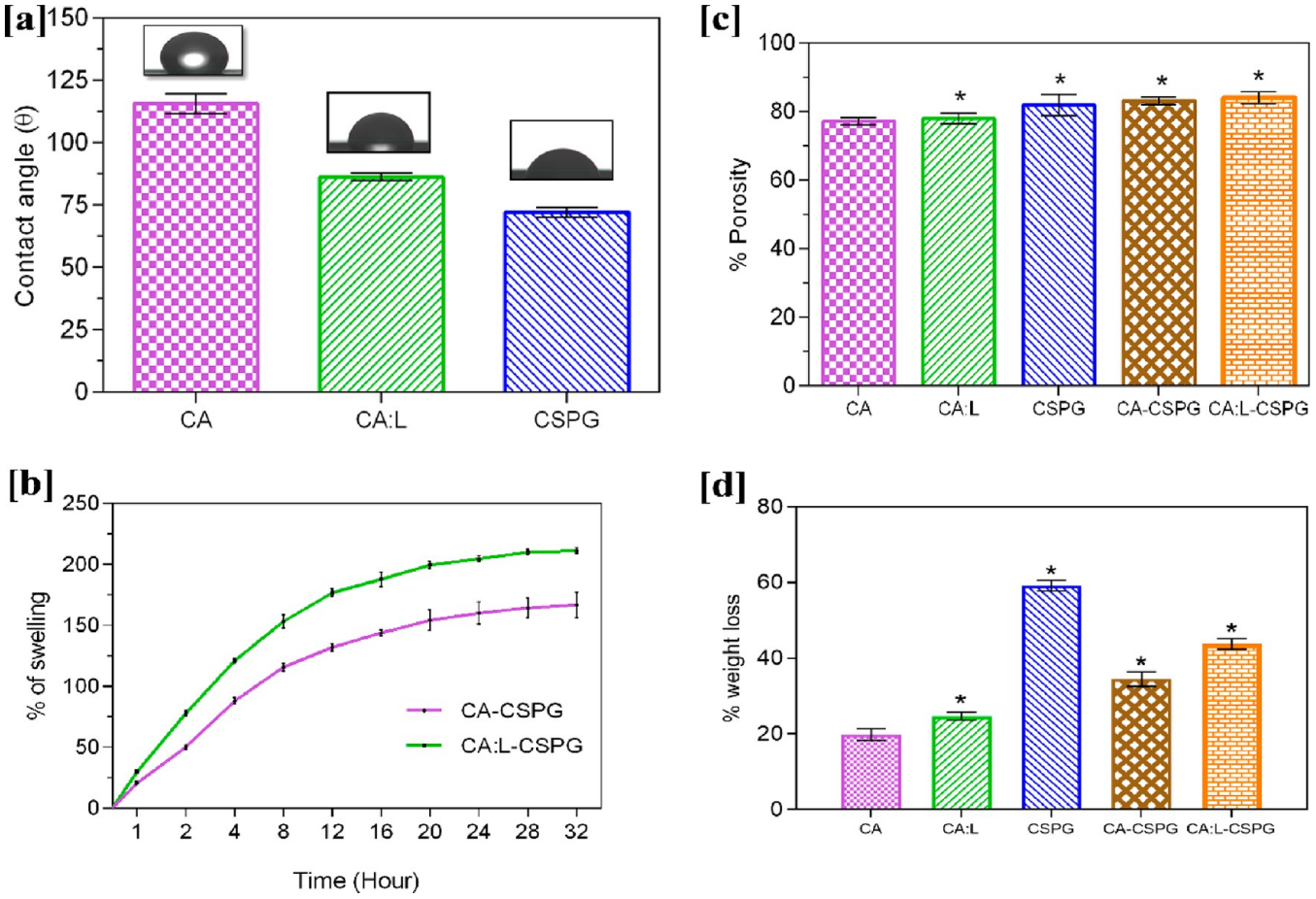

Figure 4. (a) Water contact angle of various CA, CA:L, and CSPG matrix. (b) Swelling behavior of the bilayer matrix. (c) Porosity behavior of the bilayer matrix and (d) *In vitro* enzymatic study of the bilayer matrix. All the data are represented as the mean ± SD; $n = 3$ (*$p < 0.05$).

group for acetate, and the hydroxyl groups of the polysaccharides.[40−42]

3.2. SEM Analysis. The SEM morphologies of the fabricated CA nanofibrous matrix of different concentrations are clearly shown in Figure 2. The electrospun CA nanofibre exhibited varying morphologies with different polymer concentration. Initially the 4% (w/v) solution yielded nanofibers with beaded morphology. When the concentration increased to 5% (w/v) solution, the nanofibers were smooth and uniform without any bead formation. However, at 6% (w/v) solution, the nanofiber exhibited rough and irregular surfaces as evidenced from the literature.[41] The morphology and the nature of the nanofibre serve as an essential parameter for the fabrication of biomaterial for tissue-engineering applications. However, the smooth and uniform surfaces of nanofibers are expected to support the cell adhesion and proliferation in tissue engineering.[43]

Based on the above observations, 5% (w/v) solution concentration was further selected for our studies for the incorporation of L and electrospun over the CSPG spongy material to obtain CA:L-CSPG bilayer matrix dressing material. The top and bottom surface view of the nanofibrous and spongy bilayer matrix at different magnifications are shown in Figure 3A. The top and bottom layer of the CA-CSPG and CA:L-CSPG bilayer matrix shows smooth and uniform nanofibers with highly interconnected 3D spongy surface. Moreover, the latex incorporated nanofibers exhibited excellent uniform morphology than the normal CA nanofibers. The step by step freezing of collagen before freeze-drying yields highly porous structures with increased pore sizes. Nevertheless, the partial hydrophobic nature of CA is responsible for overall biological property and stability of the bilayer matrix.

The synergistic effect from the nanofibrous and spongy morphology of the fabricated bilayer matrix was further visualized through the cross-sectional morphology shown in Figure 3B. The uniform pore size distribution of both nanofiber and spongy matrix with well interconnected pores mimics the ECM structure ensuring the exchange of gaseous and micronutrients for enhanced cell adhesion during wound healing.[11,44,10]

3.3. Contact Angle with Water, *In Vitro* Swelling Behavior, Porosity and *In Vitro* Enzymatic Degradation. *3.3.1. Contact Angle with Water.* It is essential for a biomaterial to possess hydrophilic property to influence cell viability through cell adhesion and proliferation over the nanofibrous matrix. Figure 4a shows the contact angle values of 115.6°, 86.3°, and 72° corresponding to CA, CA:L, and CSPG matrix, respectively. Here the partially hydrophobic nature of CA contributes to the increase in the contact angle. Moreover, the incorporation of L in CA:L significantly decreases the contact angle making the CA matrix hydrophilic. Further reduction of WCA value in the CSPG matrix was attributed to the hydrophilic nature of the collagen. This makes the bilayer matrix absorb more exudates during the wound healing process.[45] Thus, the synergistic effects of the bilayer matrix improve the hydrophilicity of the material for potential applications in tissue engineering.[46,41,47]

3.3.2. In Vitro Swelling Behavior. The ability of swelling is an essential property for a wound-dressing material, and it differs

https://dx.doi.org/10.1021/acs.biomac.0c00516
Biomacromolecules 2020, 21, 2512−2524

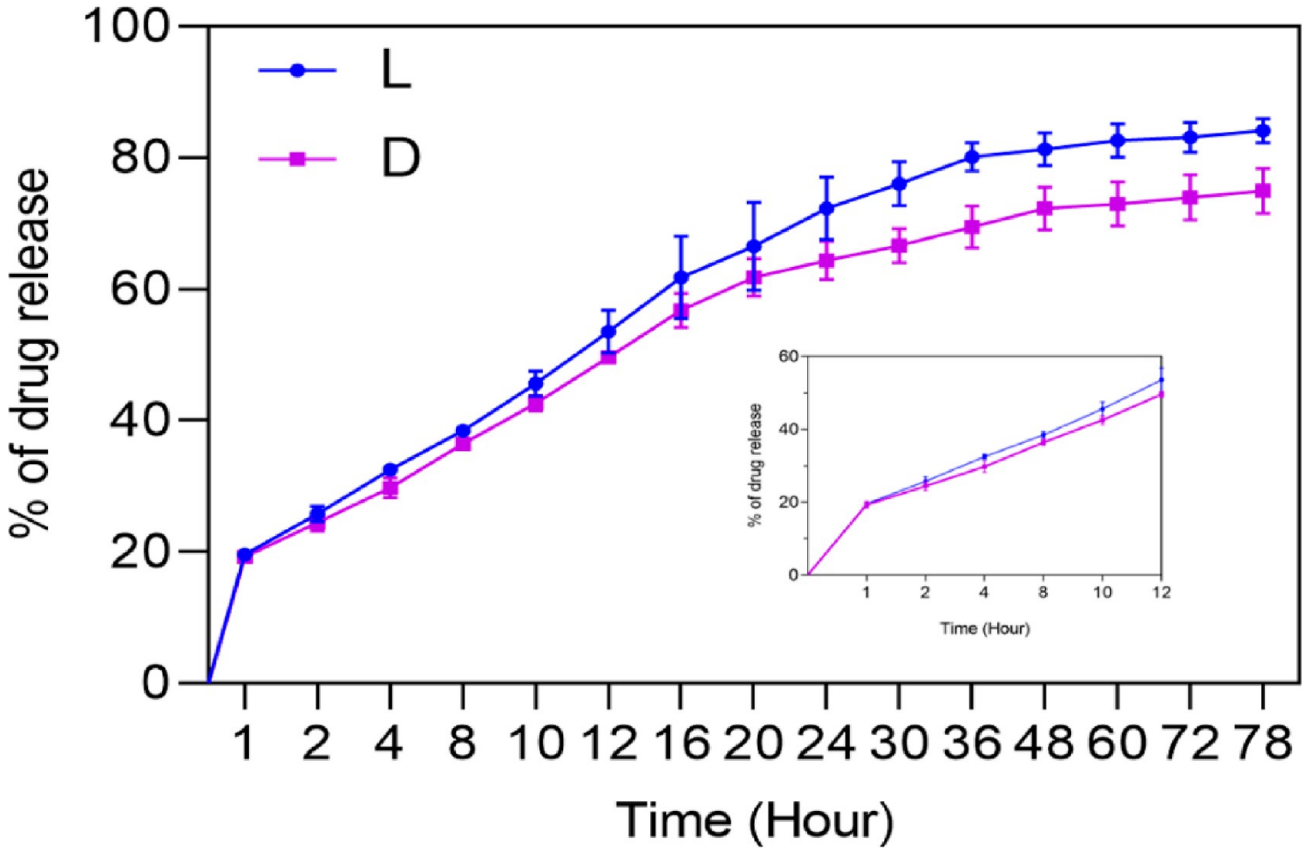

Figure 5. *In vitro* release behavior of the bilayer matrix incorporated with bioactive molecule (L) or drug (D).

from material to material. Moreover, the property of material and the fabrication of material into different forms are necessary for wound dressing to absorb the excess exudates at the wound site. The CA-CSPG and CA:L-CSPG bilayer matrix were evaluated for their swelling behavior as shown in Figure 4b. However, the existence of CA in the bilayer matrix decreases the swelling ability of the scaffold. Nevertheless, the presence of collagen on one of the layers significantly enhances the swelling of the bilayer matrix. The CA:L-CSPG matrix showed a significant difference due to the presence of latex with excellent swelling compared to CA-CSPG matrix after 24 h. Overall, the nanofibrous morphology and 3D architecture of both CA and CSPG matrix were retained without any disruption throughout the studies.[48,10]

3.3.3. Porosity. The supply and exchange of oxygen through the pores of the dressing material are essential factors in wound healing. The porosity of the material enhances the migration of the fibroblast, exchange of micronutrients, and ability to absorb the excess exudates at the wound site. The CA:L-CSPG bilayer matrix acts as a potential wound-dressing material with the ability to absorb excess exudates due to increased porosity. The porosity of CA, CA:L, CSPG, CA-CSPG, and CA:L-CSPG was assessed with a liquid displacement method and was shown in Figure 4c. In the current study, 3D architecture and nanofibrous morphology of the bilayer matrix supports the increase in porosity of the material. Moreover, the step-by-step freeze-drying process of CSPG and the incorporation of latex provides a significant increase in porosity of the bilayer matrix than CA, CA:L, and CSPG matrix in wound healing. Furthermore, both the latex incorporated CA:L-CSPG and CA-CSPG bilayer matrix possessed similar porosity. The previous study suggests that the scaffold fabricated as nanofiber[36] and spongy[10] morphology possessed to have excellent porosity than other scaffold.[11] Previous research suggests that material with uniform pore size distribution increases the porosity scaffold for tissue-engineering application.[49] Additionally, the three-dimensional space occupied by the spongy surface are eventually replace by the formation of cell in tissue-engineering application.[50] In general, a dressing material with 60−90% of cellular infiltration maintains excellent exchange of proteins and growth factors for the proliferation and migration of fibroblast in wound healing.[48,51,52]

3.3.4. In Vitro Enzymatic Degradation. Biological stability of the bilayer matrix was assessed by *in vitro* collagenase activity. The *in vitro* enzymatic degradation of the bilayer material is shown in Figure 4d. The nanofibrous spongy bilayer matrix should undergo controlled degradation at the wound site by the enzymes secreted during the process of healing. Moreover, an efficient biomaterial should demonstrate controlled biodegradation of the nanofibrous scaffold in tissue-engineering applications. The weight loss of the CSPG matrix was high when compared to the other matrices. The weight loss observed with CSPG is probably due to the degradation of collagen by the collagenase enzyme in the spongy 3D matrix.[53] The CA:L individual matrix shows an increase in weight loss when compared to the CA matrix. Moreover, the weight loss of the bilayer matrix was increased considerably because of the presence of cellulose acetate. Thus, the weight loss experienced by the individual scaffold was improved by the combination of the bilayer matrix with collagenase enzyme providing greater biological stability. Nonetheless, the synergistic effect of CA and L in the nanofibrous matrix significantly enhances the strength of the bilayer wound-dressing material.[33] Normally, dressing were changed for the open wound periodically at an interval of 4 days,[32] but given

https://dx.doi.org/10.1021/acs.biomac.0c00516
Biomacromolecules 2020, 21, 2512−2524

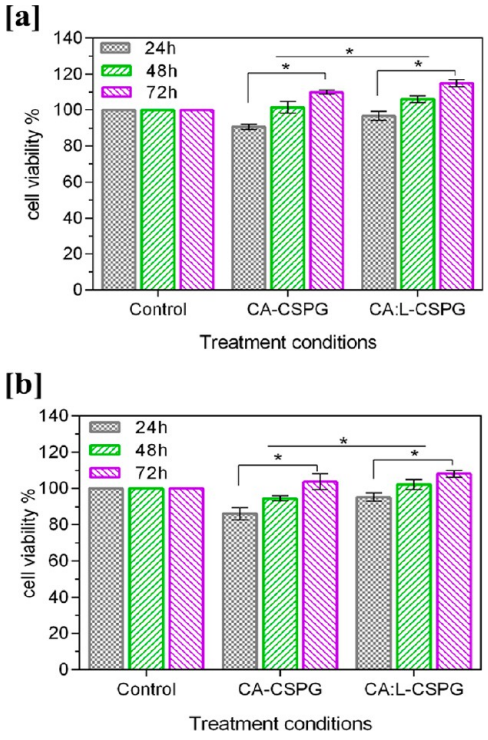

Figure 6. *In vitro* biocompatibility of the (a) NIH 3T3 fibroblast, (b) Human (HaCaT) keratinocytes cell lines over 24, 48, and 72 h using a MTT assay. The data are represented as the mean ± SD; $n = 3$ ($^*p < 0.05$).

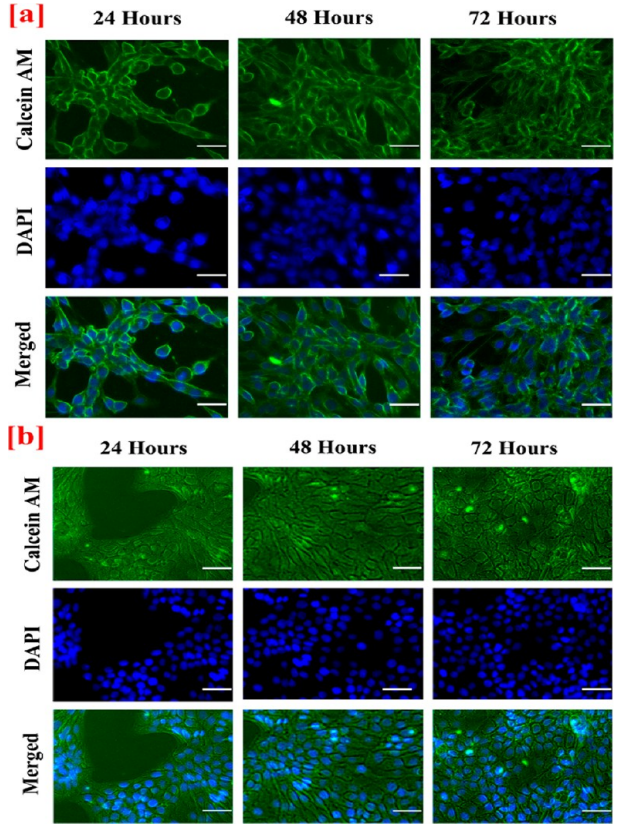

Figure 7. *In vitro* fluorescence staining images of (a) NIH 3T3 fibroblast (b) Human (HaCaT) keratinocytes cell adherence and proliferation onto the nano fibrous surface (top layer) of the CA:L-CSPG bilayer matrix at 24, 48, and 72 h. The scale bar is 100 μm.

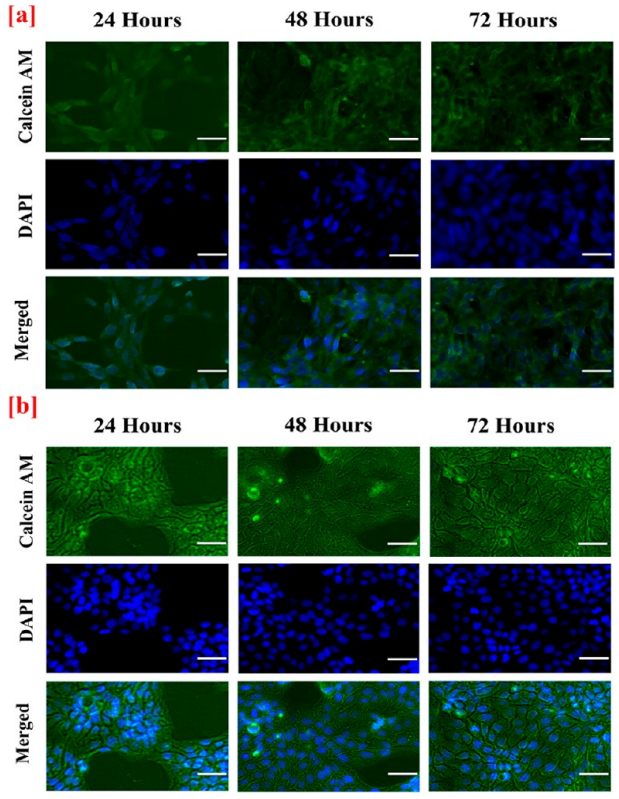

Figure 8. *In vitro* fluorescence staining images of (a) NIH 3T3 fibroblast (b) Human (HaCaT) keratinocytes cell adherence and proliferation onto the spongy surface (bottom layer) of the CA:L-CSPG bilayer matrix at 24, 48, and 72 h. The scale bar is 100 μm.

the material stability, they can be altered within a 5-day[11] period. However, the CA:L-CSPG bilayer matrix exhibited with 43.83% of degradation will favor as a suitable dressing material for wound healing application.

3.4. *In Vitro* Drug Release Study. The *in vitro* drug release study of the bilayer matrix is shown in Figure 5. The nanofibrous matrix is incorporated with bioactive molecule or drug (L and D) to act as contact layer at the wound site. The release of L and D from the bilayer matrix will prevent bacterial infection at the wound site. Burst release with 19 and 18% was observed with bilayer matrix incorporated with L and D, respectively, with the unbound surface drug. However, the decrease in the initial burst release corresponds to the drug that bounds partially to the hydrophobic nanofibrous matrix. The increase in the swelling and the porosity behavior directly proportional to the drug release in a sustained manner throughout 72 h from the bilayer CA:L-CSPG matrix.[54] Nevertheless, the sustained drug release behavior suggest the prevention of infection at wound site. However, the release of L from the primary contact layer of the bilayer matrix enhances healing with sustained drug release by acting as a suitable material in tissue-engineering application.[55,38]

Usually several mathematical models define the dissolution profile of the drug from the material. The drug release kinetics profile can be correlated with some of the mathematical models like zero-order, first-order, Higuchi and Korsmeyer−Peppas models. The *in vitro* drug release profile of both L and D was applied to different mathematical models and was interpreted from the Figures S2 and S3 and was evaluated by the correlation coefficient (r^2) represented in the Table S1. Based on the regression coefficient, the release of L and D from the nanofibrous matrix exhibits to have nearly constant release of drug directly

https://dx.doi.org/10.1021/acs.biomac.0c00516
Biomacromolecules 2020, 21, 2512−2524

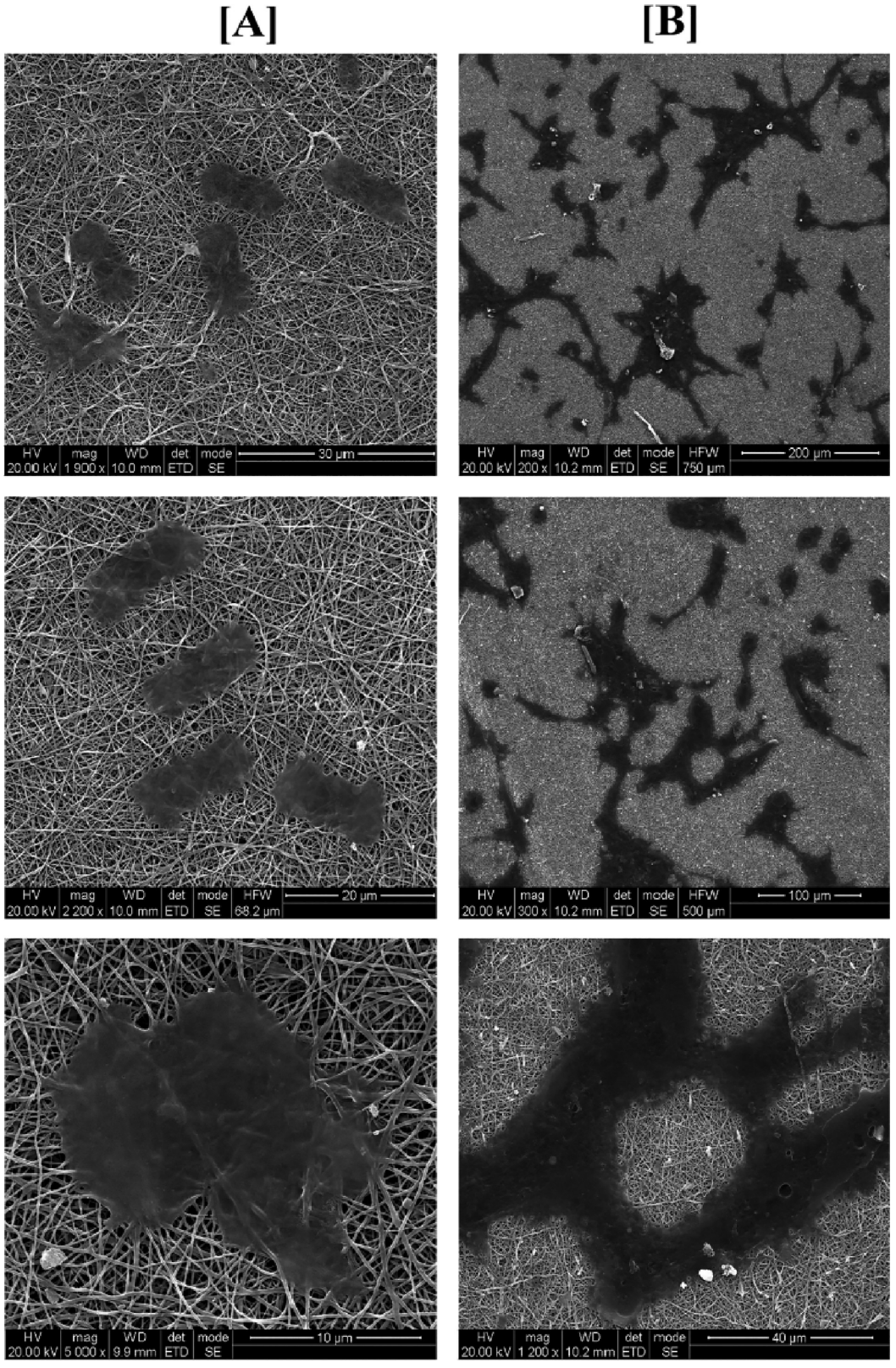

Figure 9. Scanning electron microscopy (SEM) of the cells seeded after 48 h (A) NIH 3T3 and (B) HaCaT Cells over the bilayer matrix.

proportional to the concentration of the drug loaded by following zero order and first order kinetics. However, the release of nanofibrous matrix for 78 h revealed the control release mechanism with Higuchi model. The release The Korsmeyer−Peppas plot explains the mechanism of drug diffused from the material. According to the drug release exponent (n), the nanofibrous matrix loaded with L and D follows non-Fickian diffusion (n between 0.5 to 1) and Fickian diffusion (n = 0.5) respectively. The 0.5 n value was attributed to the permeation of water into the pores of the nanofibrous matrix and make facilitates release of drugs.[56,57]

3.5. *In Vitro* Biocompatibility, Cell Adhesion, and Proliferation Studies. The development of a wound-dressing

https://dx.doi.org/10.1021/acs.biomac.0c00516
Biomacromolecules 2020, 21, 2512−2524

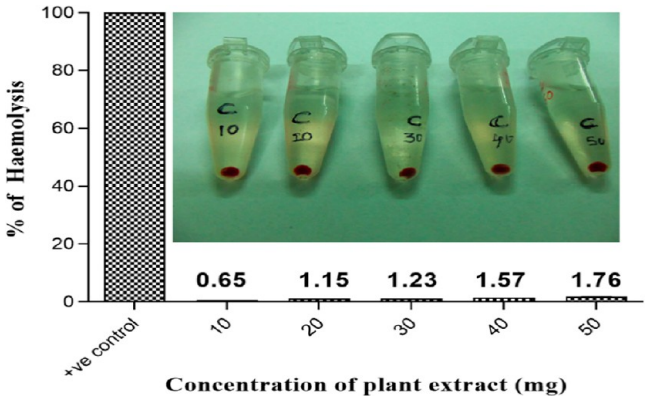

Figure 10. Hemolytic activity of the latex. Insite showing the digital image of the red blood cells exposed to various concentration of latex.

material with efficient cell adhesion and proliferation properties is highly important in tissue-engineering applications. The *in vitro* biocompatibility of CA-CSPG and CA:L-CSPG bilayer matrix were evaluated on NIH 3T3 fibroblast and HaCaT cell lines after 24, 48, and 72 h by MTT assay are shown in Figure 6a,b. The cells seeded over the nanofibrous matrix side of the bilayer scaffold exhibited increased cell viability with both cells. The CA:L-CSPG bilayer matrix showed a significant increase in cell viability than CA-CSPG bilayer matrix. The presence of latex in the nanofibrous matrix enhances the cell viability of the CA:L-CSPG bilayer matrix.[10]

The *in vitro* fluorescent staining activity of both nanofibrous layer (top layer) and spongy layer (bottom layer) of the bilayer nanofibrous matrix with Calcein AM and DAPI was evaluated with NIH 3T3 fibroblast and HaCaT cell lines after 24, 48, and 72 h. The cell adhesion and proliferation of the cells over the both nanofibrous and spongy matrix were assessed through fluorescent staining with Calcein AM and DAPI as shown in Figure 7a,b Figure 8a,b. The nanofibrous material acts as an anchoring substrate for the cells to adhere and proliferate over the nanofiber surface. In addition, the nanofibrous morphology supports the excellent stretching of cells to proliferate over the intercalated structure of the bilayer matrix with high numbers. Additionally, the spongy collagen matrix supported with good cell adhesion and proliferation. The presence of collagen attracts the migration of fibroblast, which aids in increase in cell adhesion over the bilayer matrix.[10] Nonetheless, Asaga et al. proposed that the collagen plays a unique role in the interaction of fibroblast cells for significant proliferation.[58]

The nanofibrous and spongy nature of the bilayer matrix was well supported by cell adhesion and proliferation. Moreover, the nanofibrous layer provides with excellent cell adhesion and proliferation when compared with the spongy layer of the bilayer matrix. Henceforth, the nanofibrous layer was chosen as contact surface over the wound during the wound healing application. Additionally, the cell adhesion and morphology of NIH 3T3 and HaCaT cells on the nanofibrous layer were observed under the scanning electron microscope and depicted in Figure 9a,b. The cells were spread uniformly on the nanofibrous matrix and attributed excellent biocompatibility. Nonetheless, the nanofibrous morphology of the bilayer matrix supports cell adhesion and proliferation for enhanced collagen synthesis and fast healing of the wounds. The adhesion proliferation of cells over the nanofibrous matrix was congruent with the *in vitro* fluorescence microscopy, biocompatibility, and morphology of the cells visualized through SEM analysis.[15]

3.6. *In Vitro* Antioxidant Assay, Hemocompatibility Assay, and Antimicrobial Activity of Latex (L) from *Calotropis procera*. The antioxidant studies of the *C. procera* latex exhibited with 83.14% of DPPH scavenging activity. Moreover, the reducing power and hydrogen peroxide scavenging activity showed 75.37 and 69.43%, respectively. The scavenging activity of the extract will enhance the healing during the inflammatory phase of the wound healing.[59,60] The active antioxidant property of the latex supports the formation of collagen fibrils and the proliferation of fibroblasts. The hemocompatibility of the latex was intended to be the essential assay while using the latex-loaded nanofibrous matrix at the wound site for the regeneration. The extracted latex exhibited no visible sign of hemolysis when compared to the positive control.[32] Moreover, according to the standards, samples with less than 5% are considered hemocompatible that can be evident from the Figure 10.[57] Furthermore, the antimicrobial activity of the latex significantly augments the

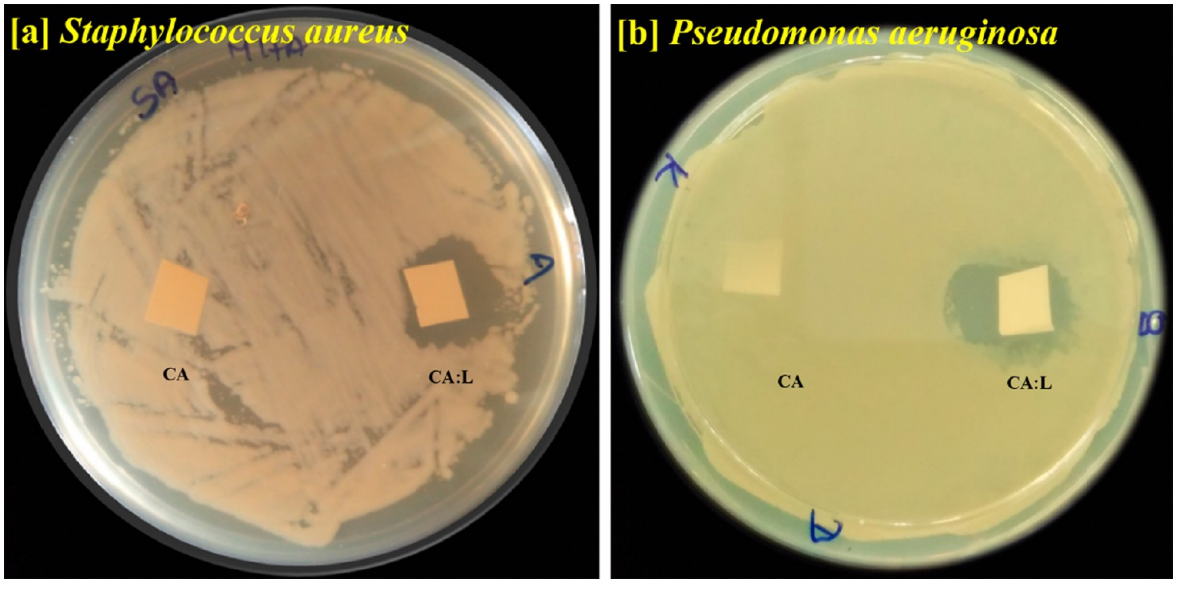

Figure 11. Antimicrobial activity of the latex incorporated CA:L matrix using (a) *Staphylococcus aureus*, (b) *Pseudomonas aeruginosa*.

https://dx.doi.org/10.1021/acs.biomac.0c00516
Biomacromolecules 2020, 21, 2512−2524

healing by keeping away from infection at wound site.[61,62] The potential antibacterial efficacy against the Gram-positive and Gram-negative bacteria were given in in Figure S3. The flavonoids and the phenolic compound present in latex as crude commensurate to the moderate zone of inhibition. The presence of the antimicrobial activity and antioxidant activity significantly will have a role in the healing and proliferation of cells, when it is incorporated into the bilayered matrix.[63]

3.7. Antimicrobial Activity of the Nanofibrous Matrix.

The bilayer nanofibrous matrix was tested for their antibacterial activity to prevent infection at the wound site, as shown in Figure 11.

The CA:L nanofibrous matrix with the bioactive latex exhibited excellent inhibition against both Gram-positive *Staphylococcus aureus* and Gram-negative *Pseudomonas aeruginosa*. The gradual release of the active molecule from CA:L nanofibrous matrix provides a zone of inhibition against the microbes. Thus, the bilayer material with CA:L at the contact layer prevents infection at the wound site and acts as a promising bilayer dressing material. Sarafdeen et al., showed the latex from the *C. procera* exhibited significant bactericidal activity than the leaf.[64] Moreover, the presence of calactin, mudarin, and calotropain as their active constituent in the *C. procera* latex plays a major role in the bactericidal activity in the nanofibrous matrix.,[65,47] The synergistic effect of the latex against the microbes was attained only by the crude nature of the latex. Moreover, the latex incorporated bilayer matrix act as dressing material topically with excellent hemocompatibility with the blood cells.[32,66]

4. CONCLUSIONS

This research work combines the synergistic effects of different materials and fabrication techniques to develop a bilayer matrix biomaterial. The CA:L-CSPG nanofibrous spongy 3D matrix act as a sustainable and promising biomaterial with excellent porosity and swelling behavior. Moreover, the bioactive latex in the bilayered matrix acts as the drug to inhibit the infection at the wound site. The 3D architecture property of the nanofibrous spongy matrix provides good cell adhesion and proliferation toward NIH 3T3 fibroblast and HaCaT cells. All these properties suggest that the developed biomaterial will serve as a promising alternative in the field of tissue-engineering applications.

■ ASSOCIATED CONTENT

Supporting Information

The Supporting Information is available free of charge at https://pubs.acs.org/doi/10.1021/acs.biomac.0c00516.

Drug release kinetics profiles, correlated with the mathematical models (Table S1, Figures S1 and S2), antimicrobial activity of the latex (Figure S3) (PDF)

■ AUTHOR INFORMATION

Corresponding Authors

Uma Tiruchirapalli Sivagnanam − *Biological Materials Lab, CSIR-Central Leather Research Institute (CLRI), Adyar, Chennai, India;* orcid.org/0000-0002-1401-2569; Email: suma67@gmail.com

Pedro Fardim − *Laboratory of Fibre and Cellulose Technology, Abo Akademi University, FI-20500 Abo, Finland; Chemical Engineering for Health & Care, Bio&Chemical Systems Technology, Reactor Engineering and Safety, Department of Chemical Engineering, KU Leuven, B-3001 Leuven, Belgium;* orcid.org/0000-0003-1545-3523; Email: pfardim@abo.fi, pedro.fardim@kuleuven.be

Authors

Giriprasath Ramanathan − *Biological Materials Lab, CSIR-Central Leather Research Institute (CLRI), Adyar, Chennai, India; Chemical Engineering for Health & Care, Bio&Chemical Systems Technology, Reactor Engineering and Safety, Department of Chemical Engineering, KU Leuven, B-3001 Leuven, Belgium;* orcid.org/0000-0002-2541-6577

Liji Sobhana Seleenmary Sobhanadhas − *Laboratory of Fibre and Cellulose Technology, Abo Akademi University, FI-20500 Abo, Finland*

Grace Felciya Sekar Jeyakumar − *Biological Materials Lab, CSIR-Central Leather Research Institute (CLRI), Adyar, Chennai, India*

Vimala Devi − *Biological Materials Lab, CSIR-Central Leather Research Institute (CLRI), Adyar, Chennai, India*

Complete contact information is available at: https://pubs.acs.org/10.1021/acs.biomac.0c00516

Author Contributions

The manuscript was written through the contributions of all the authors. All authors have approved the final version of the manuscript.

Notes

The authors declare no competing financial interest.

■ ACKNOWLEDGMENTS

The authors gratefully acknowledge The Director, CSIR-CLRI, for providing the funds and infrastructure to carry out this study. The author TSU acknowledges the financial support from Indian Council of Medical Research (ICMR) (IRIS No.2013-1293.)

■ REFERENCES

(1) Archana, D.; Dutta, P. K.; Dutta, J. Chitosan: A Potential Therapeutic Dressing Material for Wound Healing. In *Chitin and Chitosan for Regenerative Medicine*; Dutta, P. K., Ed.; Springer India: New Delhi, 2016; pp 193−227. DOI: 10.1007/978-81-322-2511-9_8.

(2) Zhang, K.; Li, Z.; Kang, W.; Deng, N.; Yan, J.; Ju, J.; Liu, Y.; Cheng, B. Preparation and Characterization of Tree-like Cellulose Nanofiber Membranes via the Electrospinning Method. *Carbohydr. Polym.* **2018**, *183*, 62−69.

(3) Ramanathan, G.; Singaravelu, S.; Raja, M.; Sivagnanam, U. T. Synthesis of Highly Interconnected 3D Scaffold from Arothron Stellatus Skin Collagen for Tissue Engineering Application. *Micron* **2015**, *78*, 28−32.

(4) Ahadian, S.; Khademhosseini, A. Smart Scaffolds in Tissue Regeneration. *Regen. Biomater.* **2018**, *5* (3), 125−128.

(5) Wang, L.; Wu, Y.; Guo, B.; Ma, P. X. Nanofiber Yarn/Hydrogel Core-Shell Scaffolds Mimicking Native Skeletal Muscle Tissue for Guiding 3D Myoblast Alignment, Elongation, and Differentiation. *ACS Nano* **2015**, *9* (9), 9167−9179.

(6) Shao, Y.; Fu, J. Integrated Micro/Nanoengineered Functional Biomaterials for Cell Mechanics and Mechanobiology: A Materials Perspective. *Adv. Mater.* **2014**, *26* (10), 1494−1533.

(7) Li, Y.; Xiao, Y.; Liu, C. The Horizon of Materiobiology: A Perspective on Material-Guided Cell Behaviors and Tissue Engineering. *Chem. Rev.* **2017**, *117* (5), 4376−4421.

(8) Tchobanian, A.; Van Oosterwyck, H.; Fardim, P. Polysaccharides for Tissue Engineering: Current Landscape and Future Prospects. *Carbohydr. Polym.* **2019**, *205*, 601−625.

(9) Zhao, R.; Li, X.; Sun, B.; Tong, Y.; Jiang, Z.; Wang, C. Nitrofurazone-Loaded Electrospun PLLA/Sericin-Based Dual-Layer Fiber Mats for Wound Dressing Applications. *RSC Adv.* **2015**, *5* (22), 16940−16949.

(10) Ramanathan, G.; Singaravelu, S.; Muthukumar, T.; Thyagarajan, S.; Perumal, P. T.; Sivagnanam, U. T. Design and Characterization of

3D Hybrid Collagen Matrixes as a Dermal Substitute in Skin Tissue Engineering. *Mater. Sci. Eng., C* **2017**, *72*, 359−370.
(11) Singaravelu, S.; Ramanathan, G.; Sivagnanam, U. T. Dual-Layered 3D Nanofibrous Matrix Incorporated with Dual Drugs and Their Synergetic Effect on Accelerating Wound Healing through Growth Factor Regulation. *Mater. Sci. Eng., C* **2017**, *76*, 37−49.
(12) Vafaei, S. R.; Tabaei, S.; Guneta, V.; Choong, C.; Cho, N.-J. Hybrid Biomimetic Interfaces Integrating Supported Lipid Bilayers with Decellularized Extracellular Matrix Components. *Langmuir* **2018**, *34* (11), 3507−3516.
(13) Horst, M.; Madduri, S.; Milleret, V.; Sulser, T.; Gobet, R.; Eberli, D. A Bilayered Hybrid Microfibrous PLGA−Acellular Matrix Scaffold for Hollow Organ Tissue Engineering. *Biomaterials* **2013**, *34* (5), 1537−1545.
(14) Singaravelu, S.; Ramanathan, G.; Muthukumar, T.; Raja, M. D.; Nagiah, N.; Thyagarajan, S.; Aravinthan, A.; Gunasekaran, P.; Natarajan, T. S.; Geetha Selva, G. V. N. Durable Keratin-Based Bilayered Electrospun Mats for Wound Closure. *J. Mater. Chem. B* **2016**, *4* (22), 3982.
(15) Cheng, M.; Qin, Z.; Hu, S.; Yu, H.; Zhu, M. Use of Electrospinning to Directly Fabricate Three-Dimensional Nanofiber Stacks of Cellulose Acetate under High Relative Humidity Condition. *Cellulose* **2017**, *24* (1), 219−229.
(16) Heinze, T.; Liebert, T. 4.2 Chemical Characteristics of Cellulose Acetate. *Macromol. Symp.* **2004**, *208* (1), 167−238.
(17) Fischer, S.; Thümmler, K.; Volkert, B.; Hettrich, K.; Schmidt, I.; Fischer, K. Properties and Applications of Cellulose Acetate. *Macromol. Symp.* **2008**, *262* (1), 89−96.
(18) Desimone, M. F.; Hélary, C.; Mosser, G.; Giraud-Guille, M.-M.; Livage, J.; Coradin, T. Fibroblast Encapsulation in Hybrid Silica−Collagen Hydrogels. *J. Mater. Chem.* **2010**, *20* (4), 666−668.
(19) Xia, Z.; Yu, X.; Jiang, X.; Brody, H. D.; Rowe, D. W.; Wei, M. Fabrication and Characterization of Biomimetic Collagen−Apatite Scaffolds with Tunable Structures for Bone Tissue Engineering. *Acta Biomater.* **2013**, *9* (7), 7308−7319.
(20) Balakrishnan, B.; Mohanty, M.; Umashankar, P. R.; Jayakrishnan, A. Evaluation of an in Situ Forming Hydrogel Wound Dressing Based on Oxidized Alginate and Gelatin. *Biomaterials* **2005**, *26* (32), 6335−6342.
(21) Zylberberg, L.; Nicolas, G. Ultrastructure of Scales in a Teleost (Carassius Auratus L.) after Use of Rapid Freeze-Fixation and Freeze-Substitution. *Cell Tissue Res.* **1982**, *223* (2), 349−367.
(22) Jin, S.; Sun, F.; Zou, Q.; Huang, J.; Zuo, Y.; Li, Y.; Wang, S.; Cheng, L.; Man, Y.; Yang, F.; et al. Fish Collagen and Hydroxyapatite Reinforced Poly(Lactide-Co-Glycolide) Fibrous Membrane for Guided Bone Regeneration. *Biomacromolecules* **2019**, *20* (5), 2058−2067.
(23) Rahman, M. A.; Wilcock, C. C. A Taxonomic Revision of Calotropis (Asclepiadaceae). *Nord. J. Bot.* **1991**, *11* (3), 301−308.
(24) Hagel, J. M.; Yeung, E. C.; Facchini, P. J. Got Milk? The Secret Life of Laticifers. *Trends Plant Sci.* **2008**, *13* (12), 631−639.
(25) Santos, A.; Van Ree, R. Profilins: Mimickers of Allergy or Relevant Allergens? *Int. Arch. Allergy Immunol.* **2011**, *155* (3), 191−204.
(26) Heli, H.; Amani, M.; Moosavi-Movahedi, A. A.; Jabbari, A.; Floris, G.; Mura, A. Electroactive Centers in Euphorbia Latex and Lentil Seedling Amine Oxidases. *Biosci., Biotechnol., Biochem.* **2008**, *72* (1), 29−36.
(27) Roy, S.; Sehgal, R.; Padhy, B. M.; Kumar, V. L. Antioxidant and Protective Effect of Latex of Calotropis Procera against Alloxan-Induced Diabetes in Rats. *J. Ethnopharmacol.* **2005**, *102* (3), 470−473.
(28) Saratha, V.; Subramanian, S.; Sivakumar, S. Evaluation of Wound Healing Potential of Calotropis Gigantea Latex Studied on Excision Wounds in Experimental Rats. *Med. Chem. Res.* **2010**, *19* (8), 936−947.
(29) Shimada, K.; Fujikawa, K.; Yahara, K.; Nakamura, T. Antioxidative Properties of Xanthan on the Autoxidation of Soybean Oil in Cyclodextrin Emulsion. *J. Agric. Food Chem.* **1992**, *40* (6), 945−948.
(30) Fejes, S.; Blázovics, A.; Lugasi, A.; Lemberkovics, É.; Petri, G.; Kéry, Á. In Vitro Antioxidant Activity of Anthriscus Cerefolium L. (Hoffm.) Extracts. *J. Ethnopharmacol.* **2000**, *69* (3), 259−265.
(31) Devendiran, R. M.; Chinnaiyan, S. K.; Mohanty, R. K.; Ramanathan, G.; Singaravelu, S.; Sobhana, S. S. L.; Sivagnanam, U. T. Sunlight Mediated Biosynthesis and Characterisation of Gold Nanoparticles Using Pisonia Grandis Leaf Extract for Biomedical Applications. *J. Biomater. Tissue Eng.* **2014**, *4* (6), 430−438.
(32) Vimala Devi, M.; Liji Sobhana, S. S.; Shiny, P. J.; Ramanathan, G.; Grace Felciya, S. J.; Poornima, V.; Thennarasu, S.; Fardim, P.; Sivagnanam, U. T. Durable Nanofibrous Matrices Augmented with Hydrotalcite-like Compounds for Cutaneous Regeneration of Burn Wounds. *Appl. Clay Sci.* **2020**, *187*, 105476.
(33) Muthukumar, T.; Senthil, R.; Sastry, T. P. Synthesis and Characterization of Biosheet Impregnated with Macrotyloma Uniflorum Extract for Burn/Wound Dressings. *Colloids Surf., B* **2013**, *102*, 694−699.
(34) Ramanathan, G.; Singaravelu, S.; Raja, M. D.; Sobhana, S. S. L.; Sivagnanam, U. T. Extraction and Characterization of Collagen from the Skin of Arothron Stellatus FishA Novel Source of Collagen for Tissue Engineering. *J. Biomater. Tissue Eng.* **2014**, *4* (3), 203−209.
(35) Ding, C.; Zhang, M.; Tian, H.; Li, G. Effect of Hydroxypropyl Methylcellulose on Collagen Fibril Formation in Vitro. *Int. J. Biol. Macromol.* **2013**, *52*, 319−326.
(36) Ramanathan, G.; Singaravelu, S.; Raja, M. D.; Nagiah, N.; Padmapriya, P.; Ruban, K.; Kaveri, K.; Natarajan, T. S.; Sivagnanam, U. T.; Perumal, P. T. Fabrication and Characterization of a Collagen Coated Electrospun Poly(3-Hydroxybutyric Acid)-Gelatin Nanofibrous Scaffold as a Soft Bio-Mimetic Material for Skin Tissue Engineering Applications. *RSC Adv.* **2016**, *6* (10), 7914.
(37) Nazarov, R.; Jin, H.-J. L.; Kaplan, D. Porous 3-D Scaffolds from Regenerated Silk Fibroin. *Biomacromolecules* **2004**, *5* (3), 718−726.
(38) Muthukumar, T.; Prabu, P.; Ghosh, K.; Sastry, T. P. Fish Scale Collagen Sponge Incorporated with Macrotyloma Uniflorum Plant Extract as a Possible Wound/Burn Dressing Material. *Colloids Surf., B* **2014**, *113*, 207−212.
(39) Babu, S. A.; Prabu, H. G. Synthesis of AgNPs Using the Extract of Calotropis Procera Flower at Room Temperature. *Mater. Lett.* **2011**, *65* (11), 1675−1677.
(40) Larkin, P. Chapter 6 - IR and Raman Spectra-Structure Correlations: Characteristic Group Frequencies. In *Infrared and Raman Spectroscopy*; Larkin, P., Ed.; Elsevier: Oxford, 2011; pp 73−115. DOI: 10.1016/B978-0-12-386984-5.10006-0.
(41) Liu, H.; Hsieh, Y.-L. Ultrafine Fibrous Cellulose Membranes from Electrospinning of Cellulose Acetate. *J. Polym. Sci., Part B: Polym. Phys.* **2002**, *40* (18), 2119−2129.
(42) Ma, Z.; Kotaki, M.; Ramakrishna, S. Electrospun Cellulose Nanofiber as Affinity Membrane. *J. Membr. Sci.* **2005**, *265* (1−2), 115−123.
(43) Lan, T.; Shao, Z.-Q.; Wang, W.-J.; Wang, F.-J.; Zhang, D.-L.; Wang, J.-Q.; Liu, Y.-H.; Kong, L.-L. Ultrafine Cellulose Triacetate Mats Electrospun by Using Co-Solvent of DMSO/Chloroform System. *J. Appl. Polym. Sci.* **2014**, *131* (12), 40373.
(44) Son, W. K.; Youk, J. H.; Lee, T. S.; Park, W. H. Electrospinning of Ultrafine Cellulose Acetate Fibers: Studies of a New Solvent System and Deacetylation of Ultrafine Cellulose Acetate Fibers. *J. Polym. Sci., Part B: Polym. Phys.* **2004**, *42* (1), 5−11.
(45) Lin, J.; Li, C.; Zhao, Y.; Hu, J.; Zhang, L.-M. Co-Electrospun Nanofibrous Membranes of Collagen and Zein for Wound Healing. *ACS Appl. Mater. Interfaces* **2012**, *4* (2), 1050−1057.
(46) Liu, J.; Lu, F.; Chen, H.; Bao, R.; Li, Z.; Lu, B.; Yu, K.; Dai, F.; Wu, D.; Lan, G. Healing of Skin Wounds Using a New Cocoon Scaffold Loaded with Platelet-Rich or Platelet-Poor Plasma. *RSC Adv.* **2017**, *7* (11), 6474−6485.
(47) Gil, C. S. B.; Gil, V. S. B.; Carvalho, S. M.; Silva, G. R.; Magalhães, J. T.; Oréfice, R. L.; Mansur, A.; Mansur, H. S.; Patricio, P. S. O.; Oliveira, L. C. A. Recycled Collagen Films as Biomaterials for Controlled Drug Delivery. *New J. Chem.* **2016**, *40* (10), 8502−8510.

https://dx.doi.org/10.1021/acs.biomac.0c00516
Biomacromolecules 2020, 21, 2512−2524

(48) Rnjak-Kovacina, J.; Wise, S. G.; Li, Z.; Maitz, P. K. M.; Young, C. J.; Wang, Y.; Weiss, A. S. Tailoring the Porosity and Pore Size of Electrospun Synthetic Human Elastin Scaffolds for Dermal Tissue Engineering. *Biomaterials* **2011**, *32* (28), 6729−6736.
(49) Chandrasekaran, A. R.; Venugopal, J.; Sundarrajan, S.; Ramakrishna, S. Fabrication of a Nanofibrous Scaffold with Improved Bioactivity for Culture of Human Dermal Fibroblasts for Skin Regeneration. *Biomed. Mater.* **2011**, *6* (1), 015001.
(50) She, Z.; Zhang, B.; Jin, C.; Feng, Q.; Xu, Y. Preparation and in Vitro Degradation of Porous Three-Dimensional Silk Fibroin/Chitosan Scaffold. *Polym. Degrad. Stab.* **2008**, *93* (7), 1316−1322.
(51) Anselme, K.; Bacques, C.; Charriere, G.; Hartmann, D. J.; Herbage, D.; Garrone, R. Tissue Reaction to Subcutaneous Implantation of a Collagen Sponge. A Histological, Ultrastructural, and Immunological Study. *J. Biomed. Mater. Res.* **1990**, *24* (6), 689−703.
(52) Loh, Q. L.; Choong, C. Three-Dimensional Scaffolds for Tissue Engineering Applications: Role of Porosity and Pore Size. *Tissue Eng., Part B* **2013**, *19* (6), 485−502.
(53) Postlethwaite, A. E.; Seyer, J. M.; Kang, A. H. Chemotactic Attraction of Human Fibroblasts to Type I, II, and III Collagens and Collagen-Derived Peptides. *Proc. Natl. Acad. Sci. U. S. A.* **1978**, *75* (2), 871−875.
(54) Peppas, N. A. Analysis of Fickian and Non-Fickian Drug Release from Polymers. *Pharm. Acta Helv.* **1985**, *60* (4), 110−111.
(55) Koo, Y.; Lee, H.; Kim, S.; Song, N.-J.; Ku, J.-M.; Lee, J.; Choi, C. H.; Park, K. W.; Kim, G. Fabrication Characterisation and in Vitro Biological Activities of a Sulfuretin-Supplemented Nanofibrous Composite Scaffold for Tissue Engineering. *RSC Adv.* **2015**, *5* (56), 44943−44952.
(56) Gandhi, A.; Jana, S.; Sen, K. K. In-Vitro Release of Acyclovir Loaded Eudragit RLPO® Nanoparticles for Sustained Drug Delivery. *Int. J. Biol. Macromol.* **2014**, *67*, 478−482.
(57) Li, W.; Peng, H.; Ning, F.; Yao, L.; Luo, M.; Zhao, Q.; Zhu, X.; Xiong, H. Amphiphilic Chitosan Derivative-Based Core−Shell Micelles: Synthesis, Characterisation and Properties for Sustained Release of Vitamin D3. *Food Chem.* **2014**, *152*, 307−315.
(58) Asaga, H.; Kikuchi, S.; Yoshizato, K. Collagen Gel Contraction by Fibroblasts Requires Cellular Fibronectin but Not Plasma Fibronectin. *Exp. Cell Res.* **1991**, *193* (1), 167−174.
(59) Tsala, D.; Nnanga, N.; Ndzana, M.; Mballa, B.; Dimo, T. Evaluation of the Antioxidant Activity and the Healing Action of the Ethanol Extract of Calotropis Procera Bark against Surgical Wounds. *J. Intercult. Ethnopharmacol.* **2015**, *4* (1), 64−69.
(60) Hsu, S. Green Tea and the Skin. *J. Am. Acad. Dermatol.* **2005**, *52* (6), 1049−1059.
(61) Lodhi, S.; Jain, A. P.; Sharma, V. K.; Singhai, A. K. Wound-Healing Effect of Flavonoid-Rich Fraction from Tephrosia Purpurea Linn. on Streptozotocin-Induced Diabetic Rats. *J. Herbs, Spices Med. Plants* **2013**, *19* (2), 191−205.
(62) Süntar, I.; Akkol, E. K.; Nahar, L.; Sarker, S. D. Wound Healing and Antioxidant Properties: Do They Coexist in Plants? *Free Radicals Antioxid.* **2012**, *2* (2), 1−7.
(63) Shobowale, O. O.; Ogbulie, N. J.; Itoandon, E. E.; Oresegun, M. O.; Olatope, S. O. A. Phytochemical and Antimicrobial Evaluation of Aqueous and Organic Extracts of Calotropis Procera Ait Leaf and Latex. *Niger. Food J.* **2013**, *31* (1), 77−82.
(64) Kareem, S.O; Akpan, I; Ojo, O.P Antimicrobial Activities of Calotropis Procera on Selected Pathogenic Microorganisms. *Afr. J. Biomed. Res.* **2008**, *11*, 105−110.
(65) Austin, D. F. Healing Plants of Peninsular India. *Econ. Bot.* **2002**, *56* (3), 292.
(66) Shobowale, O. O.; Ogbulie, N. J.; Itoandon, E. E.; Oresegun, M. O.; Olatope, S. O. A. Phytochemical and Antimicrobial Evaluation of Aqueous and Organic Extracts of Calotropis Procera Ait Leaf and Latex. *Niger. Food J.* **2013**, *31* (1), 77−82.

SPECIAL ISSUE PAPER

This paper was intended for the "Anselme Payen Award Special Issue", published May 11, 2020.

https://dx.doi.org/10.1021/acs.biomac.0c00516
Biomacromolecules 2020, 21, 2512−2524